International Journal of Recent Technology and Engineering (IJRTE)
ISSN: 2277-3878 (Online), Volume-8 Issue-2, July 2019

Design and Analyze the Effect of InGaN Nano-Material in Light Emitting Diode towards Improving the Performance of Quantum Efficiency

Shyam Sunder Manaktala, K.M.Singh

Abstract- ***The efficiency of an InGaN light-emitting diode (LED) is critically dependent on internal electric field (IEF) exhibiting in its active region. In the present work we examined the properties of the NSSP light emitters. Also we developed a novel InGaN LED structure based on a Nano-structured semi-polar (NSSP) GaN template. This new structure can be fabricated on a mature c-plane substrate including low cost sapphire without any ex situ patterning. From this approach we got results in which we can see that with the help of RT PL, 30% enhancement in IQE will be observed in NSSP MQWs as compared to c-plane planar MQWs with the help of SEM and TEM imaging tools. We have successfully ramped up an MOCVD tool for the epitaxial growth of GaN LEDs for this study.***

Index words-

I. INTRODUCTION

The advancement of the coming generation of high effectiveness light emitting diodes (LEDs) for solid state lighting takes a quantitative determination of intrinsic unit details to performance that is additional. A typical metric of optoelectronic gadgets is the output power of their emitted externally on the unit (P_{out}) measured in an integrating sphere. From there, 2 numbers determine the effectiveness of the LEDs: the wall plug efficiency (WPE) η_{wp} i.e., the ratio of electric input power to optical output power, and the outside quantum effectiveness (EQE) η_{EQE}, ratio between the figures of electrically injected carriers and externally observed photons. The WPE is connected to EQE by the voltage drop V in the unit as a result of the diode ahead voltage as well as series resistance, as $\eta_{wp} = P_{out}/VI$, wherever I may be the injected today's. In order to enhance it for a certain EQE, one involves structures with lower contact resistance as well as substantial conductivity substances and effective heat sink to keep high end below all operating conditions. η_{EQE} is readily evaluated by

$$\eta_{EQE} = P_{out}/(\omega)(I/q)$$

where ω is the photon energy and q is the electron charge. Though it just exposes the mix of non-easily separable element parameters, like carrier injection effectiveness ηinj, inner quantum effectiveness (IQE) ηIQE, along with gentle extraction effectiveness (LEE) ηextr of the LED framework, ratio between the externally emitted photons as well as the internally produced photons in the established region.

II. INGAN/GAN ACTIVE REGION ON NSSP GAN NSSP InGaN/GaN MQWs

The attributes of InGaN MQWs developed on an NSSP GaN template had been examined in comparison with MQWs grown on a planar GaN template. For the planar MQWs, a two μm-thick GaN epilayer was deposited on a c plane sapphire substrate. Subsequently, the substrate temperature was decreased to 780◦C for the development of MQWs working with a nitrogen carrier gasoline at 400 Torr reactor pressure described in Table 1. For the NSSP MQWs, practically the identical development procedures had been carried out except the insertion of HTO as well as ISST for the development of NSSP GaN. The nominal thicknesses of InGaN quantum properly plus GaN barrier are three nm as well as ten nm, respectively, as established by transmission electron microscopy (TEM). Cross sectional TEM image showing NSSP MQWs. reveals the cross sectional TEM picture of the as grown NSSP InGaN MQWs. The 3 quantum wells had been distinctly witnessed and also marked by yellow arrows. From TEM, the crystal orientation of the NSSP MQWs was proven to include 2 distinct semi polar planes. Based on theoretical calculations, IEF in either of these semi polar planes is just approximately fifteen % of which in c plane MQW. Cross sectional TEM image showing NSSP MQWs. reveals the cross sectional TEM picture of the as grown NSSP InGaN MQWs. The 3 quantum wells had been distinctly witnessed and also marked by yellow arrows. From TEM, the crystal orientation of the NSSP MQWs was proven to include 2 distinct semi polar planes. Based on theoretical calculations, IEF in either of these 2 semi polar planes is just approximately fifteen % of which in c plane MQW.

Revised Manuscript Received on 30 July 2019.
***** Correspondence Author
Shamsunder Manataklata*, Research Scholar , Dept. Of ECE , JECRC University , Jaipur, India
K M Singh, Professor, Dept. Of ECE , JECRC University , Jaipur, India.

Table 1: Summary of MQW growth condition

Layer	Growth Temp.	Reactor Pressure (Torr)	TMG Flow (µmol/min)	TMI Flow (µmol/min)	NH3 Flow (mmol/min)	V/III Ratio	Growth Rate (nm/Hr)	Thickness (nm)
UID GaN	1040	200	125	-	118	942	1270	1970
InGaN	780	400	3.9	16.1	178	8901	60	3
GaN Barrier	780	400	14.4	-	178	12427	60	10

III. PHOTOLUMINESCENCE STUDY OF NSSP INGAN/GAN MQWS

The optical qualities of NSSP MQWs were indicated by excitation and temperature reliant photoluminescence (PL) measurements. By practicing these experiments, the IQE and IEF in an NSSP energetic area are experimentally examined. Most measurements had been carried out in comparison to some polar c plane MQW test. Figure 1 exhibits the comparison of PL intensity for equally samples at room temperature (RT; 300 K). It may be observed the PL intensity of the NSSP MQWs is 3.3 times stronger than that of the polar MQWs.

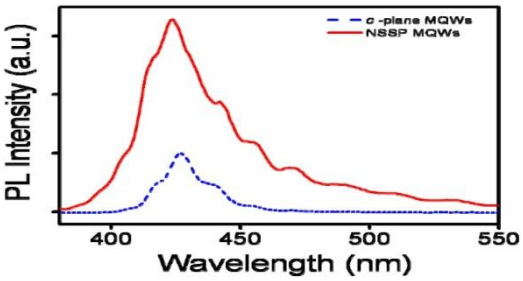

Figure 1: Photoluminescence intensity comparison of NSSP and polar MQWs at room temperature.

The PL peak wavelengths of equally samples had been assessed at different excitation intensities and shown in Figure 2. The peak wavelength of polar MQWs azure shifted when the excitation intensity increased, that had been due to the quantum confined Stark impact (QCSE) brought on by IEF. Stronger excitation raises the polarization charge screening in the quantum effectively and also lessens the IEF in polar MQWs. In comparison, the peak wavelength of NSSP stayed almost a continuous no matter improving excitation intensity, verifying the suppression of

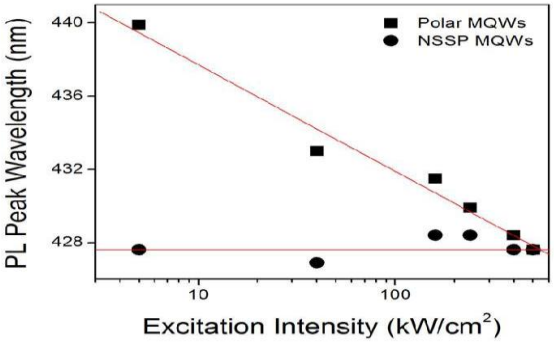

Figure 2: Photoluminescence peak wavelength as a function of excitation intensity. The two straight lines are for guides only

Figure three shows the outcomes of temperature reliant PL measurements. By assuming the IQE is unity at heat that is lower (eleven K), the IQEs of polar MQWs and NSSP could be deduced being twenty four % along with eighteen %, respectively, at five kW/cm2 excitation intensity; along with twenty % along with fifteen %, respectively, at 600 kW/cm2 excitation intensity discussed in Table 2.

The suppression of the IEF in NSSP lively area advances the IQE by about thirty %. This particular value is anticipated to be further enhanced by thorough optimizations of the development problems.

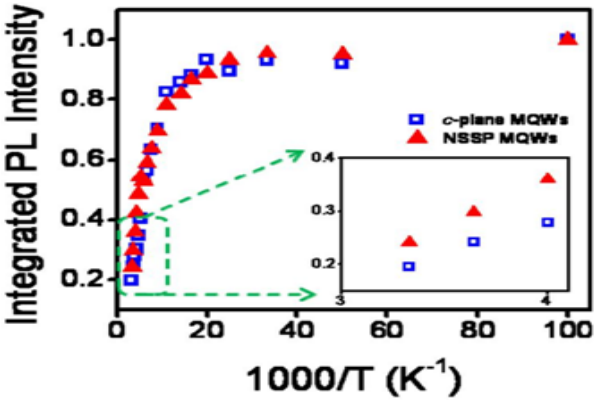

(A)

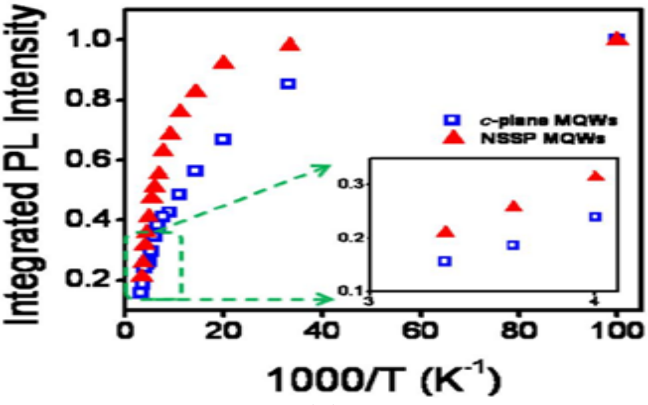

(B)

Figure 3: Arrhenius plots obtained from temperature dependent PL for NSSP and polar samples with excitation intensity of (a) 5 kW/cm² and (b) 500 kW/cm².

Table 2: IQE comparison of NSSP MQWs and polar MQWs

Excitation Intensity (kW/cm^2)	IQE of NSSP MQWs (%)	IQE of c-plane MQWs (%)	IQE Improvement of NSSP MQWs compared to c-plane MQWs (%)
5	25	19	31.6
500	21	16	31.3
Excitation Intensity (kW/cm^2)	IQE of NSSP MQWs (%)	IQE of c-plane MQWs (%)	IQE Improvement of NSSP MQWs compared to c-plane MQWs (%)
5	25	19	31.6
500	21	16	31.3

IV. TIME-RESOLVED PHOTOLUMINESCENCE STUDY OF NSSP INGAN/GAN MQWS

To additional characterize the optical qualities of an NSSP energetic region, the NSSP MQWs plus c plane polar MQWs have been examined by time resolved photoluminescence (TR PL) working with a triple frequency result associated with a mode locked titanium sapphire laser. The excitation wavelength was focused during 256 nm which has a 130 fs heartbeat wideness as well as a repetition rate of seventy five MHz. The typical laser intensity in the sample top was believed to remain one kW/cm2. The mono chrometer grating was tuned towards the good emission wavelength of each test.

To extract non-radiative and radiative lifetimes, the following formulas were used:

$$n_{Int} = \frac{1}{1 + \tau_r/\tau_{nr}}$$

$$\frac{1}{\tau_{PL}} = \frac{1}{\tau_r} + \frac{1}{\tau_{nr}}$$

Where τ_{PL}, τ_r, and τ_{nr} are PL, radiative, along with non radiative lifetimes, respectively; ηInt is IQE, that had been from the heat reliant PL measurement together with the assumption that ηInt was hundred % at temperature that is lower (twelve K). The outcomes are summarized with Table three. It may be perceived that, though the radiative lifetime was diminished significantly in the NSSP test because of the lack of QCSE, the non radiative lifetime had also been decreased. This explains why just a thirty % improvement in IQE was noticed in the NSSP test while a consideration of three changes in IQE was formerly assessed in semi polar InGaN/GaN MQWs developed on a micro scale pyramidal GaN surface area using SAE. The bodily mechanism of the reduced non radiative lifetime remains under investigation. Nevertheless, it could be partially due to the model of gallium vacancies while in the ISST operation. As the gallium vacancies weren't in the InGaN energetic region, it's thought the non radiative recombination is further minimized by optimizing the HTO problems after the ISST progression and consequently annealing the defects.

Table 3: Summary of TR PL results

	NSSP MQWs	c-plane MQWs
η_{Int}	26 %	20 %
τ_{PL}	0.17 ns	2.95 ns
τ_r	0.74 ns	16.26 ns
τ_{nr}	0.31 ns	3.62 ns

V. NSSP INGAN/GAN LEDS

1. Planarization

An electrically injected InGaN LED structure based on NSSP GaN template will be examined. After the MQW growth, a 230 nm of Mg-doped p-type GaN epilayer was deposited at 1000˚C. The p-type dopants were activated by a thermal activation process at 780 ˚C under N2 ambient for 10 minutes. The measured doping concentrations of the n-GaN and the p-GaN layers were 4 x $10^{18}/cm^3$ and 8.1 x $10^{17}/cm^3$, respectively. The growth conditions used for all layers were very similar to those used in a planar LED except for the addition of ISST and HTO processes. The entire epitaxial sequence was performed in one shot starting from a two-inch *c*-plane sapphire substrate. No electron blocking layer was included to allow us to focus the studies on the optical and electrical properties of the nano-structured active region. As shown in Figure 4, the as-grown LED surface has been mostly planarized except for a low density of micro-scale pits (3.3 x 10^5 $/cm^2$). These micro-scale pits are attributed to the threading dislocations reaching the surface although many of them disappeared during the p-GaN growth. Further optimizations of the p-GaN thickness and growth conditions are believed to be able to improve the surface morphology.

Figure 4: SEM image to show the surface morphology after p-GaN planarization

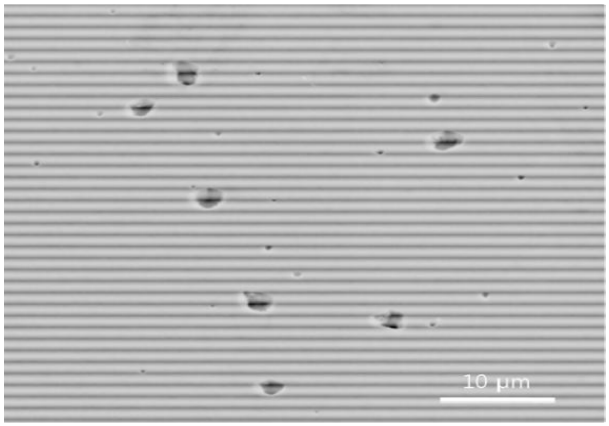

2. LED Fabrication

The mesa area was 350 µm by 350 µm and was identified by typical photolithography and also reactive ion etching (RIE; LAM 9400). A slim metallic film that comprise of five nm of Ni plus five nm of Au was deposited across the whole mesa like a transparent electrode. After the p ohmic contact development, the sample was annealed at 450 ◦C for ten minutes under N2 environment through a fast thermal annealing (RTA;

JetFirst 150 RTP). 370 nm of Au and 380 nm of Ti/Au had been deposited by an e beam evaporator as p type and n type ohmic contacts, respectively. The specifics on the LED fabrication process are revealed in the Appendix A.

VI. ELECTRICAL AND OPTICAL MEASUREMENTS

The fabricated LEDs have been indicated by regular electroluminescence (EL) measurements at room temperature with no intentional cooling. The EL spectra under a variety of continuous wave (CW) current injection are shown in Figure 5 9. The inset shows the charge coupled device (CCD) picture of the unit under current injection. Uniform light emission across the mesa was observed. The peak emission wavelength was ~ 543 nm and didn't show some azure shift with escalating current. Rather, as shown in Figure 5, the peak wavelength showed minimal white shift (< two nm over the measurement range) possibly because of Joule heating.

The full-width-half-maximum (FWHM) EL line width increased a little with escalating injection and also was much like that of semi polar green and yellow LEDs grown on semi polar bulk GaN substrates.

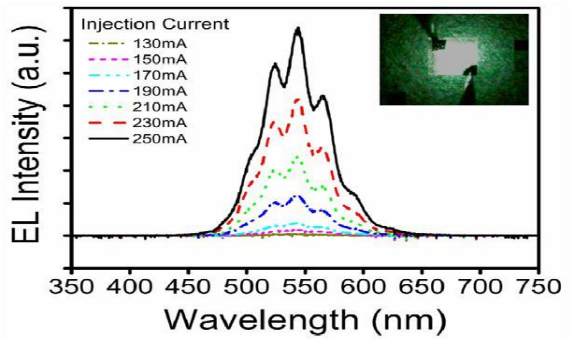

Figure 5: Electroluminescence spectra of NSSP LED for different injection currents

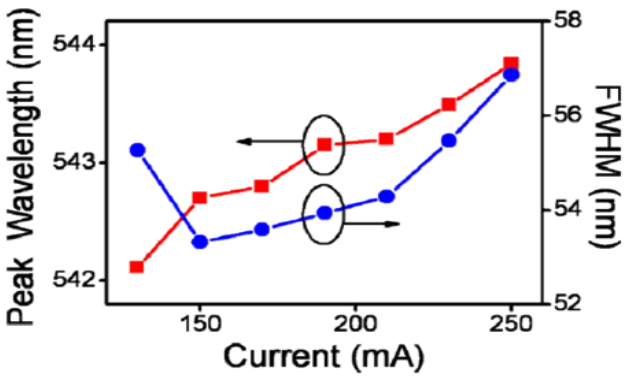

Figure 6: Peak wavelength and FWHM line width of EL spectra in NSSP LED

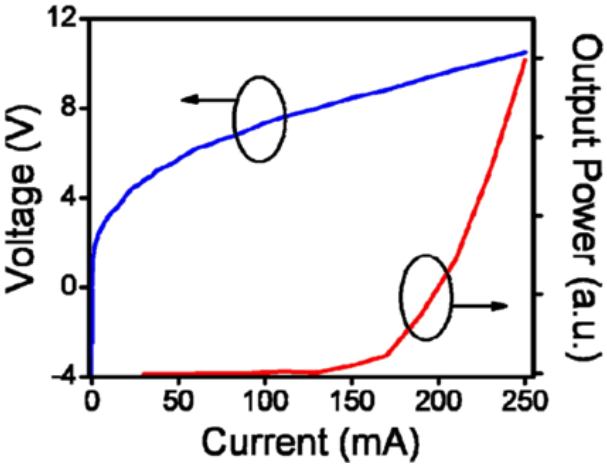

Figure 7: L-I and I-V curves of NSSP LED.

The L I as well as I V qualities of NSSP LEDs are shown in Figure 7. The turn on voltage was 4.2 V at twenty mA, which higher running voltage is due to the un optimized development problems of the NSSP template and also the p GaN present spreading layer. These micro scale pits observed on the surface area of LED (Figure 7) may also degrade the electrical properties probably because of increased contact resistance. By optimizing the p GaN level thickness as well as planarization circumstances, the development of micro scale pit is minimized and consequently the power attributes of the LED are likely to be enhanced.

VII. CONCLUSION

In this particular research, the attributes of the NSSP mild emitters were examined. Established areas have been grown on NSSP GaN beginning from a c plane sapphire substrate. From RT PL, thirty one % enhancement in IQE was noticed in NSSP MQWs as compared to c plane planar MQWs. An additional enhancement of the IQE may be possible as indicated by TRPL dimensions. We feel an optimization of HTO and ISST conditions can substantially increase non-radiative lifetime. Nano-structured semi polar LEDs have been fabricated utilizing a standard top-light-emitting framework and measured by using typical characterizations, like EL, IV, and LI. To the greatest awareness of ours, that was the very first semi polar eco-friendly LEDs raised on affordable c plane sapphire substrates. The measured EL spectra showed negligible QCSE with a peak wavelength roughly 543 nm. The EL line width was much like which of semi polar LEDs fabricated on semi polar bulk GaN substrates.

REFERENCES

1. Wang, L.; Liu, Z.; Zhang, Z.H.; Tian, Y.D.; Yi, X.; Wang, J.; Li, J.; Wang, G. Interface and photoluminescence characteristics of graphene-(GaN/InGaN)n multiple quantum wells hybrid structure. J. Appl. Phys. 2016, 119, 611–622.
2. Wang, Q.; Ji, Z.; Zhou, Y.; Wang, X.; Liu, B.; Xu, X.; Gao, X.; Leng, J. Diameter-dependent photoluminescence properties of strong phase-separated dual-wavelength InGaN/GaN nanopillar LEDs. Appl. Surf. Sci. 2017, 410, 196–200.

3. Pimputkar, S.; Speck, J.S.; Denbaars, S.P.; Nakamura, S. Prospects for LED lighting. Nat. Photonics 2009, 3, 180–182.
4. Sinnadurai, R.; Khan, M.K.A.A.; Azri, M.; Vikneswaran, V. Development of White LED down Light for Indoor Lighting. In Proceedings of the IEEE Conference on Sustainable Utilization and Development in Engineering and Technology (STUDENT), Kuala Lumpur, Malaysia, 6–9 October 2012; pp. 242–247.
5. Moon, S.; Koo, G.B.; Moon, G.W. A new control method of interleaved single-stage flyback AC–DC converter for outdoor LED lighting systems. IEEE Trans. Power Electron. 2013, 28, 4051–4062.
6. Poulet, L.; Massa, G.D.; Morrow, R.C.; Bourget, C.M.; Wheeler, R.M.; Mitchell, C.A. Significant reduction in energy for plant-growth lighting in space using targeted LED lighting and spectral manipulation. Life Sci. Space Res. 2014, 2, 43–53.
7. Sanchot, A.; Consonni, M.; Calvez, S.L.; Robin, I.C.; Templier, F. Color conversion using quantum dots on high-brightness GaN LED arrays for display application. MRS Proc. 2015, 1788, 19–21.
8. Lee, K.J. Flexible GaN LED on a polyimide substrate for display applications. Proc. SPIE 2012, 8268, 52.
9. Ferreira, R.; Xie, E.; Mckendry, J.; Rajbhandari, S. High bandwidth GaN-based micro-LEDs for multi-Gb/s visible light communications. IEEE Photonics Technol. Lett. 2016, 28, 2023–2026.